Physica A 474 (2017) 19–31

Contents lists available at ScienceDirect

Physica A

journal homepage: www.elsevier.com/locate/physa

Multi-criteria robustness analysis of metro networks

Xiangrong Wang [a,*], Yakup Koç [b], Sybil Derrible [c], Sk Nasir Ahmad [c], Willem J.A. Pino [d], Robert E. Kooij [a,e]

[a] Faculty of Electrical Engineering, Mathematics and Computer Science, Delft University of Technology, The Netherlands
[b] Systems Engineering Section, Faculty of Technology, Policy and Management, Delft University of Technology, The Netherlands
[c] Civil and Materials Engineering Department, University of Illinois at Chicago, USA
[d] Utrecht University, The Netherlands
[e] TNO South-East Asia, Singapore

HIGHLIGHTS

- We investigate the robustness of 33 real-world metro networks.
- Robustness metrics capture two distinct aspects of metros.
- Radar diagrams assess overall robustness by incorporating ten individual robustness metrics.
- Tokyo is a robust metro thanks to transfers both in the city center and the peripheral area.

ARTICLE INFO

Article history:
Received 12 July 2016
Received in revised form 2 December 2016
Available online 17 January 2017

Keywords:
Robustness
Resilience
Metro networks
Complex networks
Network metrics

ABSTRACT

Metros (heavy rail transit systems) are integral parts of urban transportation systems. Failures in their operations can have serious impacts on urban mobility, and measuring their robustness is therefore critical. Moreover, as physical networks, metros can be viewed as topological entities, and as such they possess measurable network properties. In this article, by using network science and graph theory, we investigate ten theoretical and four numerical robustness metrics and their performance in quantifying the robustness of 33 metro networks under random failures or targeted attacks. We find that the ten theoretical metrics capture two distinct aspects of robustness of metro networks. First, several metrics place an emphasis on alternative paths. Second, other metrics place an emphasis on the length of the paths. To account for all aspects, we standardize all ten indicators and plot them on radar diagrams to assess the overall robustness for metro networks. Overall, we find that Tokyo and Rome are the most robust networks. Rome benefits from short transferring and Tokyo has a significant number of transfer stations, both in the city center and in the peripheral area of the city, promoting both a higher number of alternative paths and overall relatively short path-lengths.

1. Introduction

With constant urbanization [1], cities around the world are not only growing in number but they are also growing in size. As one of the main modes of urban transportation, public transit systems are integral to move people efficiently in cities

* Corresponding author.
E-mail address: x.wang-2@tudelft.nl (X. Wang).

http://dx.doi.org/10.1016/j.physa.2017.01.072
0378-4371/

[2–4]. Indeed, they provide myriads of benefits, from reducing traffic congestion to having a lesser impact on the environment, emitting fewer greenhouse-gases per capita than the conventional automobile [5,6]. The future of public transportation is therefore bright. While increasing transit use is desirable, effort must be put into developing designs that are also resilient and robust. These subjects have gathered much interest in the scientific community in recent years, especially within the context of resilience to extreme events [7–9]. Resilience typically refers to the ability to return to a previous state after a disruption, while robustness tends to measure the amount of stress that can be absorbed before failure; Woods [10] inventoried four uses of the concept of resilience.

Traditionally, transit resilience and robustness have been associated largely with travel time reliability and variability [11]. It is still an important topic today from quantifying variability itself [12,13] or its cost [14], to using reliability and variability as a design criterion [15,16]. Recently, the field of *Network Science* [17] has emerged as particularly fitted to measure the robustness of a system, notably by studying the impact of cascading failure [18–20]. Indeed, as physical networks, metros are composed of stations (nodes) and rail tracks (links), and they therefore possess measurable network properties [21,22] that can be used to study their robustness [23–25]. Several works have also tried to combine information from both transit operation and network properties to gain insight into the robustness of transit networks [26–30].

In this work, our main objective is to analyze both theoretical and numerical robustness metrics for 33 worldwide metro systems within the realms of graph theory and network science. Metro, here, refers to heavy rail transit systems, whether underground, at grade, or overground. The freely available data from [31] was used.[1]

To assess the robustness of metros, our main research approach is to subject metros to random failures and targeted attacks. Ten theoretical robustness metrics are investigated to anticipate the influence of failures and attacks in metro networks: (i) robustness indicator r^T, see [24], (ii) effective graph conductance C_G, see [32], (iii) reliability Rel_G, see [33], (iv) average efficiency $E[\frac{1}{H}]$, see [17], (v) clustering coefficient CC_G, see [17] (vi) algebraic connectivity μ_{N-1}, see [32] (vii) average degree $E[D]$, see [32] (viii) natural connectivity $\overline{\lambda}$, see [34] (ix) degree diversity κ, see [35] (x) meshedness coefficient M_G, see [36]. Moreover, the critical thresholds $f_{90\%}$ and f_c, see for instance [37], are obtained through simulations and categorize as numerical robustness metrics which provide the ground-truth for the robustness of metros under failures and attacks.

To evaluate whether the ten theoretical robustness metrics anticipate the metros robustness with respect to node failures, we investigate the Pearson correlations between theoretical and numerical robustness metrics. The strong correlations indicate that different robustness metrics quantify different aspects of robustness and highlight the multi-faced property of the robustness of metros. Finally, an overall robustness is provided by radar diagrams that incorporate all the ten robustness metrics.

The paper is organized as follows. The definition and interpretation of theoretical robustness metrics are studied in Section 2. Section 3 presents the simulation approach for numerical robustness metrics in 33 metro networks. The performance of the robustness metrics is assessed in Section 4. Section 5 concludes the paper.

2. Theoretical robustness metrics

This section elaborates on the ten theoretical robustness metrics and how these theoretical metrics relate to robustness of networks. A physical metro network can be represented by an undirected graph $G(N, L)$ consisting of N nodes and L links. The nodes are transfer stations and terminals, while the links are rail tracks that physically join stations. A graph G can be completely represented by an adjacency matrix A that is an $N \times N$ symmetric matrix with element $a_{ij} = 1$ if there is a connection between nodes i and j, otherwise $a_{ij} = 0$. The Laplacian matrix $Q = \Delta - A$ of G is an $N \times N$ matrix, where $\Delta = \mathrm{diag}(d_i)$ is the $N \times N$ diagonal degree matrix with the elements $d_i = \sum_{j=1}^{N} a_{ij}$. The eigenvalues of Q are non-negative and at least one is zero [32]. The eigenvalues of Q are ordered as $0 = \mu_N \leq \mu_{N-1} \leq \cdots \leq \mu_1$. The degree $d_i = \sum_{j=1}^{N} a_{ij}$ of a node i is the number of connections to that node. The degree for the terminals is one.

2.1. The robustness indicator r^T

The *robustness indicator* r^T is suggested as a robustness metric for metro networks by Derrible and Kennedy [24]. It quantifies the robustness of a metro network in terms of the number of alternative paths in the network topology divided by the total number of stations in the system:

$$r^T = \frac{\mu - L^m}{N_S}$$

where N_S is the total number of stations (not limited to transfers and terminals), L^m is the number of multiple links between two nodes (e.g., overlapping lines), and μ is the cyclomatic number that calculates the total number of alternative paths in a graph; $\mu = L - N + P$, with L the number of links, N the number of nodes, and P the number of subgraphs. Transit networks are typically connected and, thus $P = 1$. The total number of stations, N_S in the denominator represents a likelihood of failure; i.e., the larger the system, the more stations need to be maintained, and therefore the more likely a station may fail.

[1] Available at http://csun.uic.edu/datasets.html, accessed July 8, 2016.

For this work, we do not consider any multiple edges.[2] Moreover, we also use the number of nodes N (i.e., transfer stations and terminals) in the denominator as opposed to the total number of stations N_S. Due to the sparsity of metro networks, i.e., $L < L_{max}$ with $L_{max} = \frac{N(N-1)}{2}$ obtained from the complete graph with N nodes, the robustness indicator in this paper is modified as:

$$r^T = \frac{\ln(L - N + 2)}{N} \tag{1}$$

where $\ln(L - N + 2)$ is employed rather than $\ln(L - N + 1)$ to avoid infinity for a tree graph with $L = N - 1$. Essentially, r^T increases when alternative paths are offered to reach a destination, and it decreases in larger systems, which are arguably more difficult to upkeep. The normalized robustness indicator $\overline{r^T}$ is obtained dividing by $r^T = \frac{\ln(L_{max}-N+2)}{N}$ with $L_{max} = \frac{N(N-1)}{2}$.

2.2. The effective graph conductance C_G

The *effective graph resistance* R_G captures the robustness of a network by incorporating the number of parallel paths (i.e., redundancy) and the length of each path between each pair of nodes. The existence of parallel paths between two nodes in metro networks and a heterogeneous distribution of each path length result in a smaller effective graph resistance and potentially a higher robustness level.

The effective resistance R_{ij} [32] between a pair of nodes i and j is the potential difference between these nodes when a unit current is injected at node i and withdrawn at node j. The effective graph resistance R_G is the sum of R_{ij} over all pairs of nodes in the network. An efficient method for the computation of the effective graph resistance in terms of the eigenvalues is

$$R_G = N \sum_{i=1}^{N-1} \frac{1}{\mu_i}$$

where μ_i is the ith non-zero eigenvalue of the Laplacian matrix.[3] Properties of the effective graph resistance are given in [32]. The effective graph resistance is considered as a robustness metric for complex networks [38], especially for power grids [39,40]. In this paper, we use a normalized version of the effective graph resistance, called the *effective graph conductance*, defined as

$$C_G = \frac{N - 1}{R_G} \tag{2}$$

where C_G satisfies $0 \leq C_G \leq 1$. Here, a larger C_G indicates a higher level of robustness. The normalized C_G enables the comparison of network robustness among different cities with different metro size.

2.3. Reliability

The *reliability* Rel_G of a network is the probability that the network is connected given the failure probabilities of its components. In this paper, we model the reliability of each link specifically as opposed to the nodes. In the absence of actual reliability data (e.g., track maintenance and age), we use a constant value for the link reliability of 0.999 in accordance with values found in the literature [41] that includes, amongst others, vehicle breakdowns, power failures, and blockage. The reliability of a link is defined as one minus the failure probability, and the method assumes that the links have independent failure probabilities. This reliability measure is used often and in various contexts [42,43], including in public transportation [44]. It essentially captures robustness by calculating the fraction of time every station is accessible from every other station. The downside of using the reliability is that it considers networks to be either fully operational or failed and does not provide any finer distinction. For further information, the reader is referred to [45].

2.4. Average efficiency $E[\frac{1}{H}]$

The hopcount H_{ij} is the number of links in the shortest path between node i and node j. The average hopcount $E[H]$ is defined as:

$$E[H] = \frac{2}{N(N-1)} \sum_{i=1}^{N} \sum_{j=1}^{N} H_{ij}.$$

When a network is disconnected, the shortest paths between certain node pairs have infinite distance. To avoid an infinitely large metric under the scenario of a disconnected graph, the global average efficiency $E\left[\frac{1}{H}\right]$ is introduced by taking

[2] Even when two stations are directly connected by multiple lines, we assign a value of 1 to the adjacency matrix. The definition is given in Section 3.1.

[3] An $N \times N$ matrix representing the graph. The definition is given in Section 3.1.

the reciprocal hopcount between two nodes [17]:

$$E\left[\frac{1}{H}\right] = \frac{2}{N(N-1)} \sum_{i=1}^{N} \sum_{j=1}^{N} \frac{1}{H_{ij}}. \tag{3}$$

Assuming the transportation efficiency between two nodes is proportional to the reciprocal of their distance, the global efficiency quantifies the efficiency of transportation in a network on a global scale.

2.5. Clustering coefficient CC_G

The clustering coefficient has become a standard in the network science literature to assess how the neighbors of a node are connected with one another. It was first introduced by [46]. The clustering coefficient of a node is defined as:

$$CC_i = \frac{2y_i}{d_i(d_i-1)}$$

where y_i is the number of links connecting neighbors of node i and d_i is the degree of node i. The clustering coefficient of a node i characterizes the connection density among the neighbors of node i. The maximum clustering coefficient is achieved in a complete graph where all the neighbors of a node are connected. In this work, we use the average clustering coefficient that is defined as the average of all individual clustering coefficients:

$$CC_G = \frac{1}{N} \sum_{i=1}^{N} CC_i. \tag{4}$$

For a graph with N nodes, the clustering coefficient is bounded by

$$0 \leq CC_G \leq 1$$

where 0 is obtained in a tree and 1 is reached in a complete graph.

2.6. Algebraic connectivity μ_{N-1}

The algebraic connectivity μ_{N-1} is the second smallest eigenvalue of the Laplacian matrix of a graph. When $\mu_{N-1} = 0$, the graph is disconnected whereas for $\mu_{N-1} > 0$ the graph is connected. It has been shown [32] that $\mu_{N-1} \leq \kappa_{\mathcal{N}}(G) \leq \kappa_{\mathcal{L}}(G)$ where $\kappa_{\mathcal{N}}(G)$ and $\kappa_{\mathcal{L}}(G)$ are node and link connectivity representing the minimum number of nodes and links whose removal disconnects the graph. Therefore, a high value of the algebraic connectivity indicates a more robust network. In addition, it implies a strong synchrony in transport networks [47] and more difficulty to break down air transport networks [48] under random failures. Because the maximum algebraic connectivity for a graph with N nodes equals N, obtained for the complete graph, we normalize by dividing the algebraic connectivity by N. The normalized algebraic connectivity is denoted as $\overline{\mu_{N-1}}$.

2.7. Average degree $E[D]$

For a graph with N nodes, the average degree can simply be written as:

$$E[D] = \frac{\sum_{i=1}^{N} d_i}{N} \tag{5}$$

where d_i is the degree of node i. Put simply, the average degree measures the number of average connections of a node. A network with a higher average degree can be thought of as more robust since it implies more connections (i.e., higher connectivity). We normalize the average degree dividing by the maximal degree, which is $N-1$, for a graph with N nodes. The normalized average degree is denoted as $\overline{E[D]}$.

2.8. Natural connectivity $\overline{\lambda}$

The natural connectivity is defined as:

$$\overline{\lambda} = \ln\left[\frac{1}{N} \sum_{i=1}^{N} e^{\lambda_i}\right] \tag{6}$$

where λ_i denote the eigenvalues of the adjacency matrix of a graph. The natural connectivity characterizes the redundancy of alternative routes and is considered as a measure of structural robustness. The natural connectivity is a monotonical function of eigenvalue λ_i that is sensitive even to a single link failure [34]. Consequently, when link failures one by one, the natural connectivity is able to capture each failure, in contrast to, for instance, link connectivity that might be the same for certain link failures. The maximum natural connectivity for a graph with N nodes is obtained in the complete graph which is $N - \ln N$ as $N \to \infty$. In order to compare graphs with different sizes, we normalize the natural connectivity, denoted as $\overline{\lambda}^*$, dividing by the maximum natural connectivity $N - \ln N$.

2.9. Degree diversity κ

The degree diversity [35], also called the second-order average degree, is defined as:

$$\kappa = \frac{\sum_{i=1}^{N} d_i^2}{\sum_{i=1}^{N} d_i}. \tag{7}$$

It has been shown that κ positively relates to the percolation threshold p_c [49] via $1 - p_c = \frac{1}{\kappa - 1}$ in the percolation model. The higher κ is, the more nodes need to be removed to disintegrate a network. In addition, the robustness of dynamic processes, e.g. epidemic spread, in a network relates to κ regarding the epidemic threshold [50], where below the epidemic threshold the network is safeguarded from long-term infection. As for homogeneous networks, such as regular graphs where each node has the same degree, the degree diversity tends to the average degree, $\kappa \to E[D]$. However, for scale-free networks with $N \to \infty$, the degree diversity tends to the infinity, $\kappa \to \infty$. In order to scale the value of the degree diversity in the interval [0, 1], we take the inverse of the degree diversity.

2.10. Meshedness coefficient M_G

The meshedness coefficient M_G is defined as:

$$M_G = \frac{L - N + 1}{2N - 5} \tag{8}$$

measuring the cycle structure in a planar graph by dividing the actual number of cycles by the potential number of cycles. It has notably been used to characterize the structural properties of urban street networks [36]. The difference between the meshedness coefficient M_G and the robustness indicator r^T lies in the denominator. The robustness indicator r^T considers the number of stations in the denominator, while M_G considers the maximal number of faces in a planar graph. The meshedness M_G satisfies $0 \leq M_G \leq 1$, where 0 is obtained in a tree graph with $L = N - 1$ and 1 is reached in the maximal planar graphs with $L = 3N - 6$.

3. Numerical robustness metrics

Numerical robustness metrics are obtained through simulations considering the robustness of 33 metro networks against random failures or deliberate attacks. This approach can be used to evaluate the performance of different robustness metrics for metro networks under node failures/attacks. This section elaborates on the metro networks, attack strategies and determination of the critical thresholds.

3.1. Metro networks

We define metros as urban rail transit systems with exclusive right-of-way whether they are underground, at grade or elevated. We represent a metro network by a graph, where nodes are transit stations and two nodes are connected if two transit stations are reachable. In this article, we look at 33 worldwide metro networks. Fig. 1 exemplifies the graphical representation of a physical metro network. Fig. 1(a) shows the map of the Athens metro network[4] and the graphical representation is shown in Fig. 1(b). In Fig. 1(b), stations 1 to 9 are respectively: Kifissia, Aghios Antonios, Attiki, Omonia, Monastiraki, Pireaus, Syntagma, Aghios Dimitrios, and Airport Eleftherios Venizelos. In this article, only the termini and transfer stations are taken into account, other stations that do not offer transfers or do not end lines are not considered as it was found preferable in [24,31]. Moreover, they tend to bias the results by simply connecting with two adjacent stations. For more details on the methodology, see [24]. Note that the methodology presented here can be readily generalized for networks including non-transfer stations by considering weighted graphs instead of unweighed graphs, where the weights equal the number of non-transfer stations between two transfer stations plus one.

3.2. Attack strategies

To determine the robustness of metro networks, the response of metro networks to targeted attacks or random failures is investigated. This paper considers two strategies for node removal: (i) random node removal and (ii) degree-based node removal.

- *Random removal:* The node to be removed is chosen at random from all the nodes in the network with equal probability.
- *Degree-based removal:* The node to be removed has the highest degree in the network. If multiple nodes have the highest degree, one node is chosen at random from all the highest-degree nodes with equal probability. In this paper, nodes are removed progressively. We first remove the node with highest degree, and continue selecting and removing nodes in decreasing order of their degree.

[4] Adapted from http://commons.wikimedia.org/wiki/File:Athens_Metro.svg.

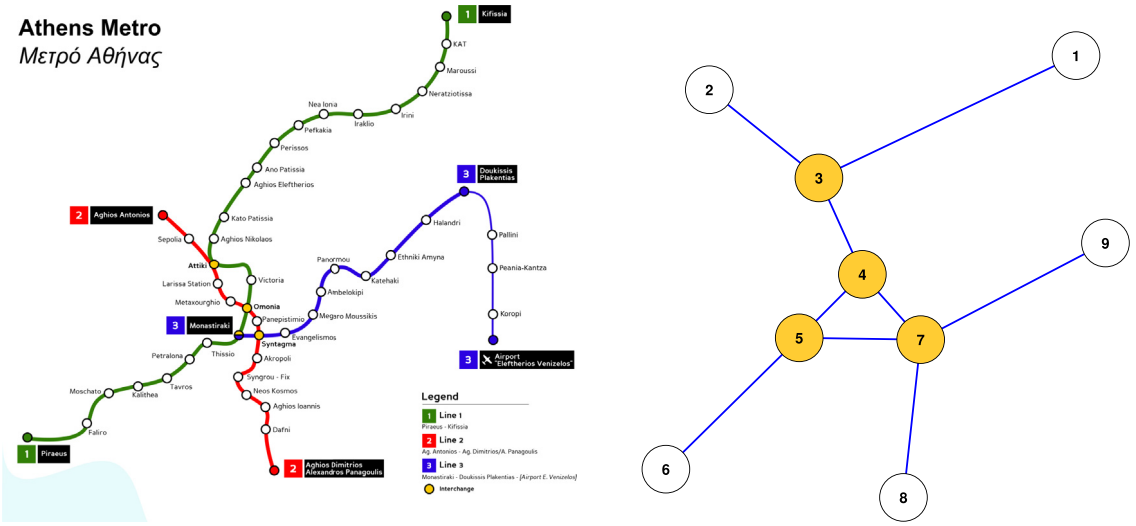

(a) The map of the Athens metro network.

(b) Graphical representation.

Fig. 1. Athens metro network.

3.3. Critical thresholds

Critical thresholds relate to the fraction of nodes that have to be removed from the network, such that the size of the largest connected component of the remaining network is equal to a predetermined fraction of the size of the original network. Critical thresholds, which are also used in the percolation model [51,52], characterize the robustness of interconnection patterns with respect to the removal/failure of network nodes.

After a node is removed, the size of the largest connected component of the remaining network is determined. Measuring the size of the largest connected component for an interval of removed nodes $[1, N]$ results in a robustness curve. From the robustness curve, we then determine the critical thresholds $f_{90\%}$ and f_c. The critical threshold $f_{90\%}$ is the first point at which the size of the largest connected component is less than 90% of the original network size. When determining the $f_{90\%}$ for random node removal, the size of the largest connected component is the average of 1000 simulation runs. Similarly, the critical threshold f_c is the first point at which the size of the largest connected component is one (i.e., the network is completely disintegrated). Fig. 2 exemplifies the determination of the critical thresholds from the robustness curve in *Tokyo* metro network with 62 nodes. Computing the size of the largest connected component for removed nodes from 1 to 62 results in a robustness curve. The size of the largest connected component is 56.77 after randomly removing 4 nodes. After removing 5 nodes, the size becomes 55.48 which is smaller than $90\% \times 62 = 55.8$, i.e., 90% of the size of the network. Therefore, the critical threshold $f_{90\%}$ is determined as $\frac{5}{62}$. The threshold f_c is determined in a similar way. The critical thresholds are regarded as the experimental robustness level of metro networks with respect to node failures.

In this paper, we first consider the threshold $f_{90\%}$, the fraction of nodes that have to be removed such that the remaining network has a largest connected component that contains 90% of the original network. For the node removal process, we simulate both random failures and targeted attacks. In the case of *random failures*, the nodes are removed by random selection, while for *targeted attacks*, the nodes are removed progressively based on their degrees (i.e., stations with many connections are removed first).

For the targeted attacks and random failures, we also consider the *critical threshold* f_c defined as the fraction of nodes to be removed such that the largest component is reduced to a size of one node (i.e., the network is completely disintegrated). As opposed to the theoretical metrics discussed in Section 2, the critical thresholds $f_{90\%}$ and f_c are obtained through simulations.

4. Metric analysis for metro networks

In this section, we study the robustness metrics for the 33 metro networks. Firstly, the ten theoretical robustness metrics are computed for the 33 metro networks. Secondly, the critical thresholds of metro networks under random failures and targeted attacks are determined by simulations. Thirdly, the relationship between the theoretical robustness metrics and numerical robustness metrics is studied. Finally, the overall performance of all the robustness metrics for the 33 metros is investigated.

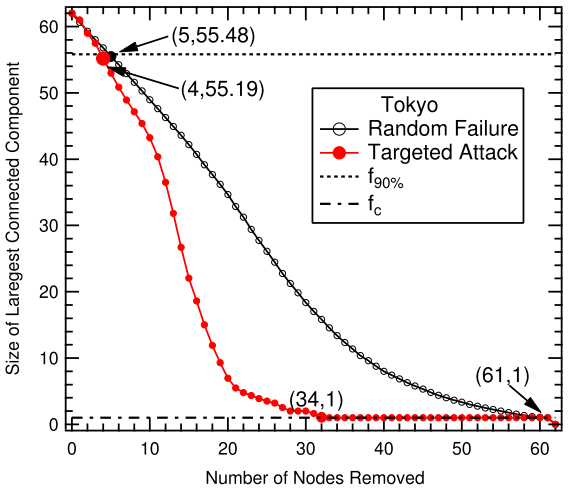

Fig. 2. The robustness curve for the Tokyo metro network.

4.1. Effectiveness of robustness metrics

Table 1 shows the values of the ten robustness metrics (from column 4 to column 13) computed using Eqs. (1)–(8) and the four numerical robustness metrics (from column 14 to column 17) using the algorithms described in Section 3.3 for the 33 metro networks.

According to the rank of the robustness indicator $\overline{r^T}$, the most robust network is *Tokyo* with $\overline{r^T} = 0.512$, followed by *Madrid* and *Paris* with $\overline{r^T} = 0.5$ and 0.488, respectively. Moreover, *Seoul*, *Moscow* and *MexicoCity* also have a relatively high robustness level. Clearly, the robustness indicator $\overline{r^T}$ favors larger networks that have developed many alternative paths between any pairs of nodes. At the same time, $\overline{r^T}$ discredits networks that have a high number of nodes while having few alternative paths. This is particularly exemplified by the case of *New York*. Due to the topography of the region, the *New York* metro lines run mostly North–South from the Bronx to Lower Manhattan and East–West in Queens and Brooklyn. The lines therefore seldom intersect as opposed to the case of the *Seoul* metro for instance.

According to the effective graph conductance C_G, *Rome* with $C_G = 0.25$ has the highest robustness level, followed by *Cairo* and *Marseille* both with $C_G = 0.17$. The effective graph conductance accounts for the number of alternative paths, but it emphasizes on the length of each alternative path. For instance, for smaller networks without cycles (e.g., star graph), the effective graph conductance increases due to the lower average path length between two stations. The topologies in Fig. 3(a) and Fig. 3(b) are particular examples. In this case, a higher effective graph conductance indicates a lower number of transfer hops between two transit stations. At the same time, effective graph conductance favors networks with the smallest length of the shortest paths. Taking Fig. 3(c) (*Montreal*) and Fig. 3(d)[5] (*Toronto*) as examples, the difference between the topologies is that station 1 connects to 10 and then connects to station 3 in *Toronto*, while stations 1 and 10 separately connect to stations 2 and 3 in *Montreal*. The total length of shortest paths from station 1 to the rest of the stations is higher in *Toronto* than in *Montreal*. Compared to *Toronto*, the higher effective graph conductance in *Montreal* indicates that the effective graph conductance favors the star-like topology with a smaller average shortest path length.

The reliability Rel_G indicates, just as the effective graph conductance does, that *Rome* is the most robust network with $Rel_G = 0.996$. After this, the most robust networks according to their reliability are *Bucharest*, *Cairo* and *Marseille*, each with $Rel_G = 0.995$. Of these three, *Cairo* and *Marseille* are also in second place according to the effective graph conductance. The reliability is sensitive to "bridges" in the network. In this work, a "bridge" is an link that if removed disconnects the network. They are of importance for the reliability because these edges must always be operational if the network is to remain a single connected component. Using this definition, we see that *Rome* has four bridges and the three networks following have five. The network with the lowest reliability is *London*. This is also the network with the most nodes and with the most bridges. Metro networks are often scale-free [24], which means that larger networks have more degree one nodes (the links to these nodes are always bridges). Therefore, it makes sense that the largest network has the highest amount of bridges and is the least reliable. Of course with different link reliabilities this line of reasoning would not hold any more.

According to the rank of $\overline{r^T}$, $\frac{1}{\kappa}$ and M_G, *Tokyo* is the most robust metro network compared to other 32 metros. Meanwhile, according to C_G, Rel_G, $E[\frac{1}{H}]$, $\overline{\mu_{N-1}}$, $\overline{E[D]}$ and $\overline{\lambda}^*$, *Rome* is the most robust metro. *Barcelona* is considered as a robust network by the clustering coefficient CC_G. *Madrid* has a relatively high robustness level favored by $\overline{r^T}$ and M_G. *Tokyo* and *Paris*

[5] In order to compare the topology of *Montreal* and *Toronto*, a link between stations 4 and 5 is added into *Toronto* and the effective graph conductance is 0.099.

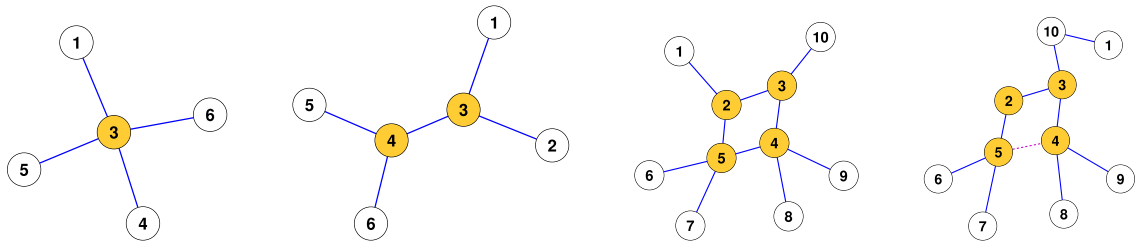

(a) Rome. (b) Cairo and Marseille. (c) Montreal. (d) Toronto.

Fig. 3. The topology of metro networks.

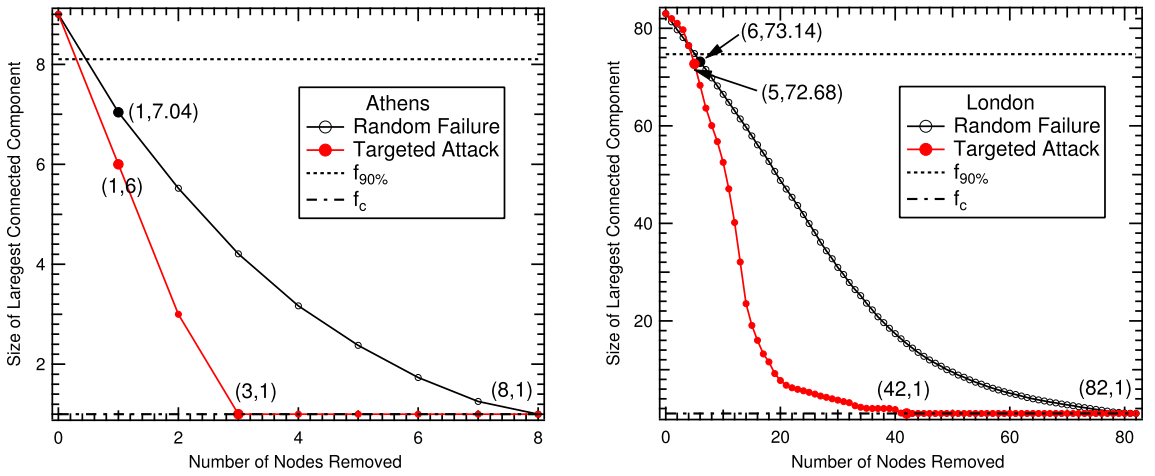

(a) Athens. (b) London.

Fig. 4. Critical thresholds in metro networks under nodes removal.

are considered as robust networks by CC_G and $\frac{1}{\kappa}$, respectively. *Cario* and *Marseille* have a relatively high robustness level regarding the second highest value of metrics C_G, Rel_G, $E[\frac{1}{H}]$, $\overline{\mu_{N-1}}$, $\overline{E[D]}$ and $\overline{\lambda}^*$. The differences in these results suggest that robustness is a multi-faceted notion, and one single measure cannot fully capture the overall robustness of a metro network.

Studying critical thresholds, Fig. 4 shows the robustness level of metro networks, taking the *Athens* and *London* metro networks as examples, under random failures and deliberate attacks. The corresponding critical thresholds $f_{90\%}$ for targeted attacks (column 14) and random failures (column 15), and f_c for targeted attacks (column 16) and random failures (column 17) are shown in Table 1. Columns 14 and 15 in Table 1 show similar behavior of $f_{90\%}$ for targeted attacks and random failures.

Similar to the effective graph conductance C_G, *Rome* has the highest robustness level with $f_{90\%} = 0.20$ both for targeted attacks and random failures. *Cairo* and *Marseille* have the second highest robustness level with $f_{90\%} = 0.17$ for both targeted attacks and random failures. In contrast, and similar to the robustness indicator r^T, an evaluation of the critical threshold f_c under targeted attacks shows that *Seoul* and *Tokyo* are the most robust networks. *Seoul* has a critical threshold $f_c = 0.76$ indicating that 76% of nodes need to be removed before the network collapses. The critical threshold f_c under random failures shows that *London*, *NewYork*, *Paris* and *Seoul* are the most robust networks.

4.2. Metric correlations

To assess the performance of theoretical metrics in capturing robustness, the Pearson correlation ρ between the ten robustness metrics and the critical thresholds in the metro networks is investigated. Moreover, the correlations within the ten robustness metrics are studied.

4.2.1. Correlation between theoretical and numerical robustness metrics

Table 2 presents the Pearson correlation between ten theoretical metrics and critical thresholds. The correlations between C_G and $f_{90\%}$ for random failures and targeted attacks are 0.89 and 0.91, respectively. The high positive correlation indicates that C_G effectively captures the 10% failure of the metro networks under node removal. Moreover, $E[\frac{1}{H}]$ and $\overline{\mu_{N-1}}$ also

Table 1
Robustness metrics in 33 metro networks.

1	2	3	4	5	6	7	8	9	10	11	12	13	14	15	16	17	18
Metros	N	L	r^T	C_G	Rel_G	$E[\frac{1}{H}]$	CC_G	$\overline{\mu_{N-1}}$	$\overline{E[D]}$	$\overline{\lambda}^*$	$\frac{1}{\kappa}$	M_G	$f_{90\%}$-degree	$f_{90\%}$-random	f_c-degree	f_c-random	Area
Athens	9	9	0.206	0.11	0.994	0.54	0.09	0.031	0.25	0.14	0.38	0.08	0.11	0.11	0.44	0.89	0.63
Barcelona	29	42	0.456	0.03	0.987	0.37	0.17	0.006	0.1	0.06	0.26	0.26	0.07	0.03	0.62	0.97	0.81
Berlin	32	43	0.417	0.03	0.986	0.36	0.08	0.005	0.09	0.05	0.28	0.2	0.09	0.06	0.56	0.97	0.45
Boston	21	22	0.209	0.03	0.984	0.37	0.03	0.005	0.1	0.06	0.34	0.05	0.05	0.05	0.43	0.95	0.17
Brussels	9	9	0.206	0.11	0.994	0.55	0.09	0.034	0.25	0.14	0.38	0.08	0.11	0.11	0.44	0.89	0.64
Bucharest	11	12	0.287	0.1	0.995	0.52	0.06	0.036	0.22	0.12	0.35	0.12	0.09	0.09	0.45	0.91	0.63
BuenosAires	12	13	0.273	0.09	0.992	0.52	0.08	0.03	0.2	0.12	0.28	0.11	0.08	0.08	0.33	0.92	0.68
Cairo	6	5	0	0.17	0.995	0.62	0	0.073	0.33	0.18	0.45	0	0.17	0.17	0.33	0.83	0.79
Chicago	25	30	0.346	0.03	0.986	0.37	0.07	0.004	0.1	0.05	0.3	0.13	0.08	0.08	0.52	0.96	0.34
Delhi	8	7	0	0.12	0.993	0.57	0	0.044	0.25	0.14	0.37	0	0.13	0.13	0.25	0.88	0.54
HongKong	17	18	0.229	0.04	0.99	0.4	0.04	0.006	0.13	0.07	0.37	0.07	0.06	0.06	0.47	0.94	0.23
Lisbon	11	11	0.181	0.09	0.993	0.52	0	0.04	0.2	0.11	0.34	0.06	0.09	0.09	0.36	0.91	0.46
London	83	121	0.455	0.01	0.966	0.24	0.1	0.001	0.04	0.02	0.27	0.24	0.06	0.07	0.69	0.99	0.44
Lyon	10	10	0.192	0.11	0.994	0.53	0	0.048	0.22	0.12	0.36	0.07	0.1	0.1	0.4	0.9	0.53
Madrid	48	79	0.5	0.03	0.988	0.32	0.13	0.003	0.07	0.04	0.25	0.35	0.08	0.1	0.67	0.98	0.77
Marseille	6	5	0	0.17	0.995	0.62	0	0.073	0.33	0.18	0.45	0	0.17	0.17	0.33	0.83	0.79
MexicoCity	35	52	0.465	0.03	0.989	0.36	0.1	0.007	0.09	0.05	0.27	0.28	0.09	0.06	0.6	0.97	0.6
Milan	14	15	0.251	0.06	0.99	0.45	0.07	0.013	0.16	0.1	0.33	0.09	0.07	0.07	0.43	0.93	0.41
Montreal	10	10	0.192	0.11	0.994	0.53	0	0.048	0.22	0.12	0.36	0.07	0.1	0.1	0.4	0.9	0.53
Moscow	41	62	0.471	0.03	0.983	0.35	0.09	0.005	0.08	0.04	0.25	0.29	0.07	0.07	0.61	0.98	0.59
NewYork	77	109	0.443	0.01	0.971	0.25	0.05	0.001	0.04	0.02	0.28	0.22	0.06	0.04	0.68	0.99	0.29
Osaka	36	51	0.443	0.03	0.988	0.34	0.08	0.004	0.08	0.04	0.28	0.24	0.08	0.06	0.61	0.97	0.47
Paris	78	125	0.488	0.01	0.975	0.27	0.13	0.001	0.04	0.02	0.24	0.32	0.08	0.06	0.71	0.99	0.66
Prague	9	9	0.206	0.12	0.994	0.57	0.06	0.061	0.25	0.15	0.33	0.08	0.11	0.11	0.33	0.89	0.76
Rome	5	4	0	0.25	0.996	0.7	0	0.2	0.4	0.22	0.4	0	0.2	0.2	0.2	0.8	1.51
Seoul	71	111	0.48	0.01	0.98	0.26	0.09	0.001	0.04	0.02	0.27	0.3	0.08	0.07	0.76	0.99	0.46
Shanghai	22	28	0.389	0.04	0.989	0.41	0.05	0.01	0.12	0.07	0.28	0.18	0.09	0.09	0.55	0.95	0.45
Singapore	12	13	0.273	0.08	0.993	0.49	0.06	0.02	0.2	0.11	0.35	0.11	0.08	0.08	0.5	0.92	0.5
StPetersburg	14	16	0.317	0.07	0.992	0.49	0.07	0.026	0.18	0.1	0.31	0.13	0.07	0.07	0.43	0.93	0.56
Stockholm	20	19	0	0.02	0.981	0.34	0	0.003	0.1	0.05	0.4	0	0.05	0.05	0.4	0.95	0.05
Tokyo	62	107	0.512	0.02	0.985	0.31	0.15	0.002	0.06	0.03	0.23	0.39	0.08	0.06	0.71	0.98	0.88
Toronto	10	9	0	0.07	0.991	0.47	0	0.018	0.2	0.1	0.45	0	0.1	0.1	0.5	0.9	0.26
WashingtonDC	17	18	0.229	0.04	0.988	0.41	0.04	0.01	0.13	0.07	0.35	0.07	0.06	0.06	0.47	0.94	0.24

Table 2
Pearson correlation ρ between theoretical robustness metrics and the critical thresholds.

	$f_{90\%}$-degree	$f_{90\%}$-random	f_c-degree	f_c-random
$\overline{r^T}$	−0.41	−0.52	0.87	0.85
C_G	0.89	0.91	−0.82	−0.97
Rel_G	0.54	0.59	−0.72	−0.75
$E[\frac{1}{H}]$	0.76	0.81	−0.9	−0.96
CC_G	−0.41	−0.52	0.73	0.66
$\overline{\mu_{N-1}}$	0.86	0.85	−0.71	−0.85
$\overline{E[D]}$	0.83	0.87	−0.87	−0.99
$\overline{\lambda}^*$	0.81	0.85	−0.88	−0.98
$1/\kappa$	0.56	0.64	−0.74	−0.83
M_G	−0.43	−0.53	0.89	0.8

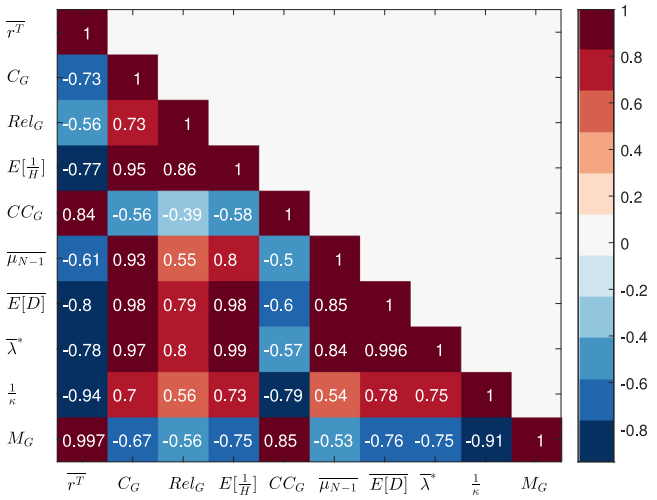

Fig. 5. Pearson correlation ρ between theoretical robustness metrics.

characterize the 10% failure of metro networks with performance slightly lower than C_G. The reliability Rel_G positively, but less strongly, correlates with critical thresholds $f_{90\%}$. However, the above mentioned metrics negatively correlate with f_c ($\rho(C_G, f_c) = -0.82$ for targeted attacks and $\rho(C_G, f_c) = -0.97$ under random failures).

The high correlation between $\overline{r^T}$ and f_c shows that $\overline{r^T}$ effectively characterizes when the network collapses under node removal. One explanation for the high correlation between $\overline{r^T}$ and f_c is that the robustness indicator $\overline{r^T}$ and the critical threshold f_c both characterize the number of alternative paths. Besides $\overline{r^T}$, the correlations of metrics M_G and CC_G to f_c suggest that these metrics have comparable performance in capturing when the network collapses. Yet, the correlations of $\overline{r^T}$, M_G and CC_G to $f_{90\%}$ are negative.

Metrics that positively correlate with $f_{90\%}$ and those that positively correlate with f_c therefore capture different aspects of metro networks as hinted above, and both are important for robustness. Redundancy and contradiction between theoretical metrics are observed when capturing robustness of metros under node removal. Redundancy means that more than one metric positively correlates with critical thresholds and contradiction means that one specific metric positively correlates to $f_{90\%}$ while negatively correlates to f_c and vice versa.

4.2.2. Correlation within theoretical robustness metrics

To analyze the redundancy and contradiction of metrics, the Pearson correlation ρ between all the theoretical robustness metrics is investigated in Fig. 5. In Fig. 5, C_G, $E[\frac{1}{H}]$, $\overline{\mu_{N-1}}$ and Rel_G that effectively capture the critical threshold $f_{90\%}$ show a higher mutual correlation (e.g. $\rho\left(C_G, E[\frac{1}{H}]\right) = 0.95$). Similarly, for metrics $\overline{r^T}$, M_G and CC_G that capture the critical threshold f_c, a higher mutual correlation result is observed (e.g. $\rho\left(\overline{r^T}, CC_G\right) = 0.84$).

As shown in Fig. 5, these robustness metrics have a higher mutual correlation which indicates redundancy in capturing the robustness. Correspondingly, a representative set of robustness metrics by including only one metric from the mutually strongly depend set of metrics tends to sufficiently and effectively characterize the robustness [35]. For example, when quantifying the robustness $f_{90\%}$, including C_G in the representative set is more sufficient and effective than including C_G, $\overline{\mu_{N-1}}$ and $E[\frac{1}{H}]$.

In contrast to the positive and high correlations between certain metrics, the negative correlations in Fig. 5 (e.g. −0.73 between $\overline{r^T}$ and C_G) might be problematic. In particular, when a higher $f_{90\%}$ and f_c are desired in the design of a metro, optimizing, for instance, both the robustness metrics $\overline{r^T}$ and C_G is beyond reach. Because maximizing $\overline{r^T}$ minimizes C_G and vice versa. This is therefore a major issue, which is not atypical of any robustness study. Indeed, while it is easy to develop design recommendations that can make a system more robust to certain conditions, it is much more challenging to develop recommendations that can make a system more robust overall. This point emphasizes the need to use multiple criteria when assessing the design of metro networks. It also points to the fact that robustness (and *resilience* more generally) are terms that are difficult to define and that cannot be solved with a simple objective function within an operation research context [53]. Instead, much work remains to be done to successfully come up with clear guidelines to transit planners, and simulation and network science may play an important part towards that end.

A possible approach to deal with this issue is suggested by Van Mieghem *et al.* [54], who defined a *R*-value, which is a weighted sum of all the considered theoretical metrics, i.e., *R*-value $= \sum_{i=1}^{M} w_i m_i$, where w_i is the weight for each metric m_i and M is the number of metrics taken into account. In the next subsection, we discuss another approach, which is based upon radar diagrams that are commonly used in urban planning and geography.

4.3. Overall robustness

To combine the ten calculated theoretical metrics that capture different aspects of robustness, we choose to draw radar diagrams for each metro. A radar diagram (also called star or spider diagram) is plot with as many axes as there are metrics, and the overall performance is calculated by measuring the area of the polygon formed. This type of diagram is especially useful when it is not possible to assign weights to individual metrics. First, for each set of metrics, each individual value x_i is being rescaled to a value in the interval [0, 1] using the rescaling formula: $(x_i - x_{min})/(x_{max} - x_{min})$. In the radar diagram, the robustness metrics are placed in a clockwise order. Metrics that are positively correlated with the critical threshold $f_{90\%}$ are located on one side and metrics that are negatively correlated to the critical threshold $f_{90\%}$ are placed on the other side.

Fig. 6 shows the radar plots for the 33 metro networks.[6] Moreover, Table 1 (last column) contains the areas of the polygons calculated. Overall, we can see that *Rome* and *Tokyo* are the top two of the most robust networks. Tokyo has many transfer stations in the periphery of the network that both enables it to offer many alternative paths and keep a relatively low resistance, hence ensuring a robust system. At the other hand of the spectrum, *Stockholm*, *Boston* and *Hong Kong* (the three least robust metros) have extensive networks with few transfer stations that inherently affect their robustness. Even *Washington DC* does not perform well because the transfer stations tend to be located in the city center, and it therefore achieves poorly in terms of "resistance" (i.e., long many stations without transfer from the terminals in the suburbs to the city center).

Most other networks tend to perform somewhat in between. From Fig. 6, networks with polygons that are large in the bottom right corner tend to have many alternative paths. In contrast, metros with polygons that are large in the left-hand side tend to perform well in terms of resistance (as is the case for *Rome* despite its simple topology). *Mexico City* and *Berlin* deserve special attention since they seem to perform well in nearly all dimensions. *Berlin* has a particularly dense U-Bahn system, and *Mexico City* is known to have L-shaped lines to favor transferring [55].

From this work, clear recommendations can be set to promote a robust metro:

- Transfer stations are desirable to offer alternative paths. However, although large hubs are desirable to facilitate transferring, smaller hubs are as desirable to offer more options to transfer, thus offering more alternative paths (moreover they are less vulnerable to targeted attacks than large hubs).
- Long line sections are undesirable since a failure on one station will affect many passengers, likely resulting in the need for an emergency bus service to substitute failed stations. Transfer stations can therefore be located strategically to offer alternative paths while ensuring that line segments without transfer stations are kept as short as possible.

5. Conclusion

The main objective of this work was to investigate the robustness of metro networks by analyzing several robustness metrics. In particular, we study ten theoretical robustness metrics and four numerical metrics. For the latter, we investigated two critical thresholds f, when 90% of the network is still remaining, $f_{90\%}$, and when the complete network is disintegrated, f_c (both under random failure and targeted attack).

Overall, we find that the ten theoretical robustness metrics capture two distinct aspects of the robustness of metro networks. A first aspect deals with the number of alternative paths, suggesting that more alternative paths is more desirable, as captured in r^T. In contrast, the second aspect deals with "resistance", suggesting that longer lines with no shorter alternative paths perform poorly, as captured in C_G. Essentially, as metro networks are expanded, effort should be put into creating transfer stations, both in city centers and peripheral areas to ensure that not only many alternative paths are created to reach a destination, but also that the average number of stations between two transfers is kept to a minimum. Overall we found that *Rome* benefits from shorter transferring paths and *Tokyo* are able to accomplish more transferring options.

[6] The degree diversity κ instead of $\frac{1}{\kappa}$ is used in the radar diagram for the simplicity of computing the area.

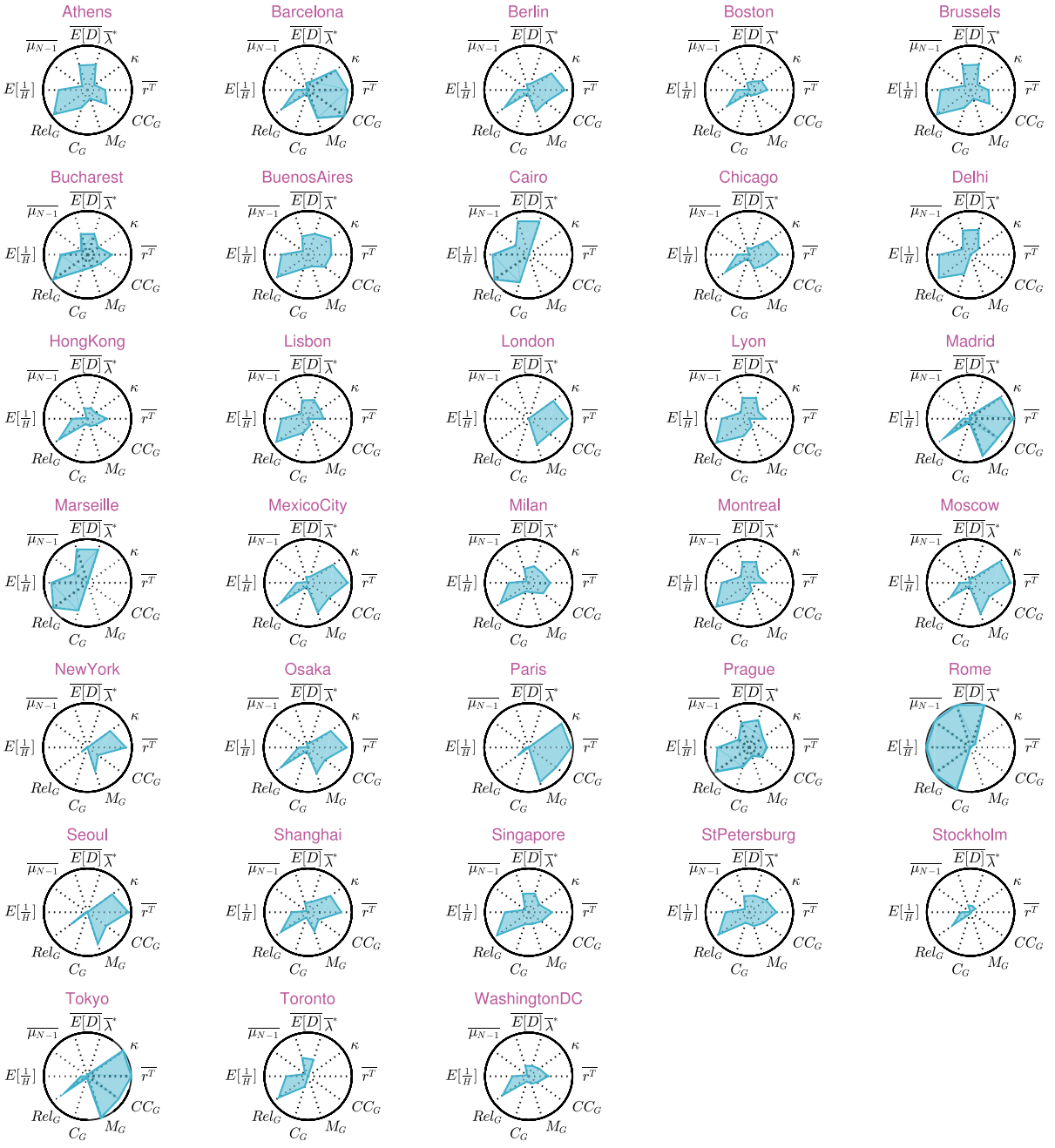

Fig. 6. Radar diagrams for the 33 Metro Networks.

Based on these observations and to fully capture these two aspects and assess the robustness of metro networks, we plotted the ten theoretical measures (standardized) on radar plots. This method offers both an equal representation of the variables at play as well as aesthetically-pleasing visual aid to help planners in their task to design robust metro networks.

Acknowledgment

This research is supported by the China Scholarship Council (CSC).

References

[1] United Nations, World Urbanization Prospects: The 2014 Revision, United Nations, New York, ISBN: 978 -92-1-151517- 6, 2014.
[2] V.R. Vuchic, Urban Transit Systems and Technology, John Wiley & Sons, 2007.

[3] S. Derrible, Urban infrastructure is not a tree: integrating and decentralizing urban infrastructure systems, Environ. Plan. B: Plan. Des. (2016).
[4] S. Derrible, Complexity in future cities: the rise of networked infrastructure, Int. J. Urban Sci. (2016) 1–19.
[5] S. Derrible, S. Saneinejad, L. Sugar, C. Kennedy, Macroscopic model of greenhouse gas emissions for municipalities, Transp. Res. Rec.: J. Transp. Res. Board 2191 (2010) 174–181.
[6] C.D. Cottrill, S. Derrible, Leveraging big data for the development of transport sustainability indicators, J. Urban Technol. 22 (1) (2015) 45–64.
[7] B.M. Ayyub, Systems resilience for multihazard environments: Definition, metrics, and valuation for decision making, Risk Anal. 34 (2) (2014) 340–355.
[8] W. Cai, S. Borlace, M. Lengaigne, P. Van Rensch, M. Collins, G. Vecchi, A. Timmermann, A. Santoso, M.J. McPhaden, L. Wu, et al., Increasing frequency of extreme el niño events due to greenhouse warming, Nature Clim. Change (2014).
[9] A. Kermanshah, S. Derrible, A geographical and multi-criteria vulnerability assessment of transportation networks against extreme earthquakes, Reliab. Eng. Syst. Saf. 153 (2016) 39–49.
[10] D.D. Woods, Four concepts for resilience and the implications for the future of resilience engineering, Resilience Engineering 141 (2015) 5–9 (special issue).
[11] H.S. Levinson, The reliability of transit service: An historical perspective, J. Urban Technol. 12 (1) (2005) 99–118.
[12] L.M. Kieu, A. Bhaskar, E. Chung, Public transport travel-time variability definitions and monitoring, J. Transp. Eng. 141 (1) (2015).
[13] E. Mazloumi, G. Currie, G. Rose, Using gps data to gain insight into public transport travel time variability, J. Transp. Eng. 136 (7) (2010) 623–631.
[14] V. Benezech, N. Coulombel, The value of service reliability, Transp. Res. B 58 (2013) 1–15.
[15] B. Yao, P. Hu, X. Lu, J. Gao, M. Zhang, Transit network design based on travel time reliability, Transp. Res. C 43 (2014) 233–248.
[16] K. An, H.K. Lo, Service reliability based transit network design with stochastic demand, in: Transportation Research Board 93rd Annual Meeting, Number 14-1971, 2014.
[17] M.E.J. Newman, Networks: An Introduction, Oxford University Press, 2010.
[18] D.J. Watts, A simple model of global cascades on random networks, Proc. Natl. Acad. Sci. 99 (9) (2002) 5766–5771.
[19] P. Crucitti, V. Latora, M. Marchiori, Model for cascading failures in complex networks, Phys. Rev. E 69 (4) (2004) 045104.
[20] R. Kinney, P. Crucitti, R. Albert, V. Latora, Modeling cascading failures in the north American power grid, Eur. Phys. J. B 46 (1) (2005) 101–107.
[21] S. Derrible, C. Kennedy, A network analysis of subway systems in the world using updated graph theory, Transp. Res. Rec. 2112 (2009) 17–25.
[22] S. Derrible, C. Kennedy, Characterizing metro networks: State, form, and Structure, Transportation 37 (2) (2010) 275–297.
[23] B. Berche, C. von Ferber, T. Holovatch, Y. Holovatch, Resilience of public transport networks against attacks, Eur. Phys. J. B 71 (1) (2009) 125–137.
[24] S. Derrible, C. Kennedy, The complexity and robustness of metro networks, Physica A 389 (17) (2010) 3678–3691.
[25] C. von Ferber, B. Berche, T. Holovatch, Y. Holovatch, A tale of two cities: Vulnerabilities of the London and Paris transit networks, J. Transp. Secur. 5 (3) (2012) 199–216.
[26] E. Rodríguez-Núñez, J.C. García-Palomares, Measuring the vulnerability of public transport networks, J. Transp. Geogr. 35 (0) (2014) 50–63.
[27] H. Kim, C. Kim, Y. Chun, Network reliability and resilience of rapid transit systems, Prof. Geogr. (2015) 1–13.
[28] X. Wang, Y. Koç, S. Derrible, S.N. Ahmad, R.E. Kooij, Quantifying the robustness of metro networks, in: 6th International Symposium on Transportation Network Reliability, Nara, Japan, 2015.
[29] O. Cats, E. Jenelius, Dynamic vulnerability analysis of public transport networks: Mitigation effects of real-time information, Netw. Spat. Econ. 14 (3–4) (2014) 435–463.
[30] O. Cats, E. Jenelius, Planning for the unexpected: The value of reserve capacity for public transport network robustness, Transp. Res. A 81 (2015) 47–61.
[31] S. Derrible, Network centrality of metro systems, PloS ONE 7 (7) (2012) e40575.
[32] P. Van Mieghem, Graph Spectra for Complex Networks, Cambridge University Press, Cambridge, UK, 2011.
[33] C.J. Colbourn, The Combinatorics of Network Reliability, vol. 200, Oxford University Press New York, 1987.
[34] J. Wu, M. Barahona, Y.J. Tan, H.Z. Deng, Spectral measure of structural robustness in complex networks, IEEE Trans. Syst. Man Cybern. A 41 (6) (2011) 1244–1252.
[35] C. Li, H. Wang, W. De Haan, C.J. Stam, P. Van Mieghem, The correlation of metrics in complex networks with applications in functional brain networks, J. Stat. Mech. Theory Exp. 2011 (11) (2011) P11018.
[36] A. Cardillo, S. Scellato, V. Latora, S. Porta, Structural properties of planar graphs of urban street patterns, Phys. Rev. E 73 (6) (2006) 066107.
[37] R. Cohen, S. Havlin, Complex Networks: Structure, Robustness and Function, Cambridge University Press, 2010.
[38] X. Wang, E. Pournaras, R.E. Kooij, P. Van Mieghem, Improving robustness of complex networks via the effective graph resistance, Eur. Phys. J. B 87 (9) (2014) 1–12.
[39] Y. Koç, M. Warnier, P. Van Mieghem, R.E. Kooij, F.M.T. Brazier, The impact of the topology on cascading failures in a power grid model, Physica A 402 (2014) 169–179.
[40] X. Wang, Y. Koç, R.E. Kooij, P. Van Mieghem, A network approach for power grid robustness against cascading failures, in: 7th International Workshop on Reliable Networks Design and Modeling, IEEE, 2015, pp. 208–214.
[41] M.D. Yap, Robust Public Transport From a Passenger Perspective: A Study to Evaluate and Improve the Robustness of Multi-Level Public Transport Networks (Master's thesis), Delft University of Technology, 2014.
[42] M.L. Rebaiaia, D. Ait-Kadi, Network Reliability Evaluation and Optimization: Methods, Algorithms and Software Tools, Interuniversity Research Center on Enterprise Networks, Logistics and Transportation, 2013.
[43] M.O. Ball, C.J. Colbourn, J.S. Provan, Network reliability, in: Handbooks in Operations Research and Management Science, vol. 7, 1995, pp. 673–762.
[44] S. Tahmasseby, Reliability in Urban Public Transport Network Assessment and Design, TU Delft, Delft University of Technology, 2009.
[45] J. Carlier, C. Lucet, A decomposition algorithm for network reliability evaluation, Discrete Appl. Math. 65 (1) (1996) 141–156.
[46] D.J. Watts, S.H. Strogatz, Collective dynamics of 'small-world' networks, Nature 393 (6684) (1998) 440–442.
[47] R.K. Kincaid, N. Alexandrov, M.J. Holroyd, An investigation of synchrony in transport networks, Complexity 14 (4) (2009) 34–43.
[48] P. Wei, G. Spiers, D. Sun, Algebraic connectivity maximization for air transportation networks, IEEE Trans. Intell. Transp. Syst. 15 (2) (2014) 685–698.
[49] R. Cohen, K. Erez, D. Ben-Avraham, S. Havlin, Resilience of the internet to random breakdowns, Phys. Rev. Lett. 85 (21) (2000) 4626.
[50] Y. Moreno, R. Pastor-Satorras, A. Vespignani, Epidemic outbreaks in complex heterogeneous networks, Eur. Phys. J. B 26 (4) (2002) 521–529.
[51] M.E.J. Newman, I. Jensen, R.M. Ziff, Percolation and epidemics in a two-dimensional small world, Phys. Rev. E 65 (2) (2002) 021904.
[52] D.S. Callaway, M.E.J. Newman, S.H. Strogatz, D.J. Watts, Network robustness and fragility: Percolation on random graphs, Phys. Rev. Lett. 85 (25) (2000) 5468.
[53] N. Taleb, Antifragile: Things That Gain from Disorder, Random House Publishing Group, New York, NY, 2012.
[54] P. Van Mieghem, C. Doerr, H. Wang, J. Martin Hernandez, D. Hutchison, M. Karaliopoulos, R.E. Kooij, A Framework for Computing Topological Network Robustness, Technical Report 20101218, Delft University of Technology, 2010.
[55] R. Cervero, The Transit Metropolis: A Global Inquiry, Island Press, 1998.